# SPIRE FLIGHT

# THERMAL MODEL CORRELATION REPORT

| THERMAL ENGINEERING GROUP | | | | |
|---|---|---|---|---|
| PREPARED BY | A.S. GOIZEL | (RAL) | 20-03-07 | pp ? Signature Not Verified Digitally signed by Bryan Shaughnessy Date: 2007.03.21 11:33:51 Z |
| CHECKED BY | B. SHAUGHNESSY | (RAL) | | ? Signature Not Verified Digitally signed by Bryan Shaughnessy Date: 2007.03.21 11:34:06 Z |
| **SPIRE PROJECT** | | | | |
| APPROVED BY | E. SAWYER | (RAL) | | ? Signature Not Verified Digitally signed by Eric Sawyer Date: 2007.03.26 11:11:29 +01'00' |

*"Page intentionally left blank"*

## CHANGE RECORD

| Issue | Date | Section | Change |
|---|---|---|---|
| Draft A | 15/09/06 | - | New Document. |
| Draft B | 14/03/07 | All | Complete missing sections |
| Issue 1 | 20/03/07 | - | First Issue |

# CONTENTS

*1 Introduction* *6*

**1.1 Scope** **6**

**1.2 Acronyms** **6**

*2 DocumentS* *7*

**2.1 Applicable Documents** **7**

**2.2 Reference Documents** **7**

*3 Thermal Characterisation/Correlation of SPIRE* *9*

**3.1 Correlation Overview** **9**

**3.2 Limitations** **9**

**3.3 Thermal Models** **10**

**3.4 Validation of 300mK system level** **10**
3.4.1 Cooler during Low Temperature Operation Phase 10
3.4.2 Sorption Cooler Model – Hold time Predictions 11
3.4.3 300mK Busbar Assembly 12
3.4.4 Bolometer Detector Arrays 14

**3.5 Validation of the L0 Detector Enclosure Stage** **16**
3.5.1 L0 Interbox Strap and SST L0 Supports Parasitic Load 16
3.5.2 Flight CFRP L0 Supports and Parasitic Load 21

**3.6 Validation of the Flight L0 Thermal Straps** **23**

**3.7 Validation of Instrument Power Dissipation at L1** **24**
3.7.1 PCAL Operation 24
3.7.2 SCAL Operation 24
3.7.3 SMEC Operation 25
3.7.3.1 Definition of Operating Modes 25
3.7.3.2 Verification of SMEC PFM Coil Resistance 25
3.7.3.3 Verifications of SMEC PFM Power Dissipation 26
3.7.4 BSM operation 27

**3.8 Validation of L1 Parasitic Load** **29**

**3.9 Validation of JFET Boxes Performance** **29**

# LIST OF TABLES

Table 1-1– Acronym List 6
Table 2-1- Applicable Documents 7
Table 2-2 - Reference Documents 8
Table 3-1 – Correlated Cooler TMM Predictions versus Cooler Performances measured at Unit Level 11
Table 3-2- Measured versus Predicted Cooler Hold Time for Unit Level Testing 12
Table 3-3 – Predicted Photometer BDAs temperature for PFM2 13
Table 3-4 – Updated Predictions for Photometer BDAs temperature for PFM2 13
Table 3-5 – Predicted Photometer BDAs temperature for PFM3 13
Table 3-6 – Updated Predictions for Photometer BDAs temperature for PFM3 14
Table 3-7 – BDA Internal Parasitic Load Correlation 15
Table 3-8– BDA Internal Temperature Drop Correlation 15
Table 3-9 – Heater Test Setup for L0 Enclosure Characterisation 17
Table 3-10 - Interbox L0 Strap Characterisation Test – Results 17
Table 3-11 – G1 and G2 overall conductances versus temperature 18
Table 3-12 – Stycast Glued Joint Interface Conductance curve fit 18
Table 3-13 – Nominal Temperature and conductance used for iteration 19
Table 3-14 - Degradation Factor: 0.588 – two similar values are obtained for Qp (data converged) 19
Table 3-15 – SPIRE Thermal Model Correlation of CFRP L0 Supports Conductance for Cold Case 22
Table 3-16 -SPIRE Thermal Model Correlation of CFRP L0 Supports Conductance for Hot Case 22
Table 3-17 – Predicted thermal conductance of the SPIRE L0 Thermal Straps 23
Table 3-18 – PCAL Operation during PFM3 test campaign [RD9] 24
Table 3-19 – SCAL2 Operation during PFM3 test campaign [RD9] 24
Table 3-20 – SCAL2 Operation during PFM3 test campaign [RD9] 24
Table 3-21- SMEC Scanning Modes 25
Table 3-22 - SMEC Current vs Displacement Linear Law 26
Table 3-23 – SMEC Peak Current in MED and LO Resolution Scanning Mode 26
Table 3-24 – SMEC Average Power Dissipations 27
Table 3-25 – PFM BSM Performance 27
Table 3-26 – PJFET Correlation Overview 29

# LIST OF FIGURES

Figure 3-1 – L0 Interbox Strap Conductance ..... 20
Figure 3-2 –Thermal Conductivity of CFRP used by MSSL for design of L0 and L1 Supports ..... 21
Figure 3-3 – SMEC Current, Voltage and Power Dissipation in High Resolution Scan Mode [RD12] ..... 25
Figure 3-4 - SMEC Current, Voltage and Scan Position in MED and LO Resolution Scan Modes [RD12]..... 26
Figure 3-5 - 7 point jiggle AOT performed during PFM4 ..... 27
Figure 3-6 – BSM Power Dissipation at Chop and Jiggle Combinations [RD14]..... 28

# 1 INTRODUCTION

## 1.1 Scope

This report summarises the correlation work which has been completed for the detailed thermal mathematical model of the SPIRE flight model.

## 1.2 Acronyms

| *Acronym* | *Definition* |
|---|---|
| AD | Applicable Document |
| BDA | Bolometer Detector Arrays |
| BSM | Beam Steering Mechanism |
| CBB | Cold Black Body |
| CQM | Cryogenic Qualification Model |
| DRCU | Digital Readout Control Unit |
| DTMM | Detailed Thermal Mathematical Model |
| EGSE | Electronic Ground Support Equipment |
| FM | Flight Model |
| FPU | Focal Plane Unit |
| FS | Flight Spare |
| HCSS | Herschel Common Science System |
| HeI | Helium I |
| HeII | Helium II |
| HOB | Herschel Optical Bench |
| I/F | Interface |
| IIDB | Instrument Interface Document Part B |
| IRD | Instrument Requirement Document |
| ILT | Instrument Level Testing |
| JFET | Junction Field Effect Transistor |
| L0 | Level-0 |
| L1 | Level-1 |
| L2 | Level-2 |
| L3 | Level-3 |
| LN2 | Liquid Nitrogen |
| MGSE | Mechanical Ground Support Equipment |
| PFM | Proto Flight Model |
| RD | Reference Document |
| SMEC | Spectrometer Mechanism |
| SCU | Subsystem Control Unit |
| SOB | SPIRE Optical Bench |
| SPIRE | Spectral and Photometric Imaging Receiver |
| TBT | Thermal Balance Test |

*Table 1-1– Acronym List*

# 2 DOCUMENTS

## 2.1 Applicable Documents

| ID | Title | Number |
|---|---|---|
| AD1 | SPIRE Thermal Design Requirements | SPIRE-RAL-PJR-002075 |
| AD2 | SPIRE Instrument Interface Document Part B (IIDB) | SPIRE-ESA-DOC-000275 |

*Table 2-1- Applicable Documents*

## 2.2 Reference Documents

| RD | Title | Number |
|---|---|---|
| RD1 | SPIRE FM1 Sorption Cooler EIDP<br>Section 6 – Interface and Top Level Drawings | HSO-SBT-ADP-108<br>Issue 1 |
| RD2 | SPIRE Sorption Cooler FM1 Test Report | HSO-SBT-RP-118<br>Issue 1 |
| RD3 | SPIRE PFM2 Thermal Performance Flight Predictions | SPIRE-RAL-NOT-002588<br>Issue 1 |
| RD4 | SPIRE 300-mK and Level-0 straps Subsystems Thermal Performances Assessment | SPIRE-RAL-NOTE-002129<br>Issue 1 |
| RD5 | RE: RAL Assumptions for BDA Thermal Model | Emaill from Inseob Hahn<br>06/05/03 |
| RD6 | PFM PLW BDA SN014 HRCR PACKAGE preliminary.pdf<br>PFM PMW BDA SN012 HRCR PACKAGE_preliminary.pdf<br>PFM PSW BDA SN013 HRCR PACKAGE preliminary.pdf<br>PFM SLW BDA SN008 HRCR PACKAGE_preliminary.pdf<br>PFM SSW BDA SN009 HRCR PACKAGE_preliminary.pdf | PFM BDA EIDPs |
| RD7 | SPIRE CQM1/2 Thermal Test Balance Report | SPIRE-RAL-REP-002078<br>Issue 1 |
| RD8 | SPIRE PFM2 Thermal Balance Test Report | SPIRE-RAL-REP-002534<br>Issue 1 |
| RD9 | SPIRE PFM3 Thermal Balance Test Report | SPIRE-RAL-REP-002684<br>Issue 1 |
| RD10 | SPIRE Verification Science Review Thermal Performance | SPIRE-RAL-REP-002557<br>Issue 2 |
| RD11 | Flight L0 Thermal Strap Conductance – Unit Level Test Results | See Pete Hargrave Emails On 20/02/07, 27/02/07 and 07/03/07. |
| RD12 | SPIRE PFM4/PFM5 Thermal Balance Test Report | SPIRE-RAL-REP-002784<br>Issue 1 |
| RD13 | SMEC CQM Cryogenic Test Results | LAM.ELE.SPI.PRV.040731<br>_01, edition 1 rev 0 |

| | | |
|---|---|---|
| RD14 | PFM BSM Unit Level Performance testing | Bryan Stobie's email on 09/02/04 |

*Table 2-2 - Reference Documents*

# 3 THERMAL CHARACTERISATION/CORRELATION OF SPIRE

## 3.1 Correlation Overview

The SPIRE instrument underwent a total of 6 instrument level test campaigns at RAL (in addition to the subsystems unit level testing). A number of reports have been produced (RD7 to RD9) each summarising the outcomes and results of thermal tests carried out during these test campaigns.

Each thermal test has been devised to allow the correlation and/or verification of a specific aspect of the thermal design or instrument performance. The correlation of the SPIRE thermal model is therefore based on test data from various test campaigns.

Please note that the PFM4 and PFM5 test campaigns have not been used for the correlation of the model (with the exception of the SMEC power dissipation). The cooler hold time and detectors performance were checked to confirm the instrument was working as expected (based on the performance characterised as part of the PFM2 and PFM3 test campaigns).

## 3.2 Limitations

It is important to note that the correlation exercise was made difficult for the following reasons:

- The calibration cryostat was designed to provide SPIRE with a nominal 1.7K-4.2K thermal environment but it was not optimised to perform accurate thermal characterisation of the instrument (i.e. small heat loads monitored on highly conductive thermal straps, adjustment of the thermal environment limited).

- A number of corrective actions have been implemented which have help the correlation process (i.e. heat sinking of cryo-harnesses, integration of a manostat for the control of the L0 temperature stage, addition of more temperature sensors, and addition of GSE heater on the L0 photometer enclosure).

- A basic thermal model of the calibration cryostat was developed but it has never been correlated as such. There is a certain level of uncertainty regarding the environmental loads SPIRE is subjected to while in operation in the cryostat and there is also some uncertainty as to how repeatable this environment is from one test campaign to the other (harness heat sinks, helium leaks, and stray light from 77K shield).

- Issues with EGSE thermometry – despite best efforts to repair/exchange faulty temperature sensors, sensors were regularly lost during each test campaign making cross-correlation from one to the other very difficult.

- Calibration issue with the flight temperature sensors – during the PFM2 test campaign, it was demonstrated that DC offsets are present on the flight thermometry (flight and redundant). These “calibration” errors have been present during all test campaigns and cannot be corrected for in hardware. As a result, any data from the flight thermometry could not confidently be used for thermal correlation of the model unless it was specifically read out on the GSE AC bridge.

## 3.3 Thermal Models

The SPIRE instrument thermal model which has been used for this analysis can be found on the Thermal_Models network drive at the Rutherford Appleton Laboratory under (unless otherwise specified):
\\Thermal_Models\TD-01-02-SPIRE\DTMM\ DTMM\SPIRE_TMM_STAL_3-2

The thermal model logfile can be found at:
\\Thermal_Models\TD-01-02-SPIRE\DTMM\ SPIRE_TMM_STAL_Logfile.xls

The SPIRE stand-alone model [SPIRE_TMM_STAL_3-2] sets certain nodes as boundaries while disabling others according to test cases which allow the correlation of a specific aspect of the model.

## 3.4 Validation of 300mK system level

### *3.4.1 Cooler during Low Temperature Operation Phase*

An important aspect of the cooler thermal model correlation is the validation of the cooler total parasitic load during the low temperature operation phase at 300mK. This depends on the following parameters:

- Evaporator Kevlar support, from 4K to 0.3K,
- Evaporator to Shunt Titanium Tube, from 1.7K to 0.3K,
- Evaporator Heat Switch OFF conductance, from 1.7K to 0.3K.

The thermal model of the cooler was updated to reflect the changes from the CQM cooler to the FM cooler based on the following reports [RD1] and [RD2].

The cooler thermal model correlation was based on test data from the cooler Unit Level Testing (ULT) [RD2].

The following thermal model was used for the correlation:
J:\TD-01-02-SPIRE\DTMM\SPIRE_TMM_STAL_3-1\SPIRE_TMM_FM_2-4s1.d

A report of the correlation approach and results can be found in [RD3], a summary of the important assumptions and correlation results is repeated here for information.

The following uncertainties are applicable when assessing the cooler performance [RD2]:

- The cooler Helium charge has been estimated to be 6.3L at +/-5%,
- A 6.3L helium charge has been assumed for the theoretical predictions,
- When the cooler runs out of helium, there is no sharp temperature rise and thus it will be assumed that the cooler has run out of helium as soon as its evaporator temperature has risen by 1%,
- A +/-3.3% correlation was achieved by Lionel Duband between the measured and predicted hold time of the flight cooler during unit level testing.
- A similar level of agreement should therefore be expected between performance predicted with the TMM and performance measured as part of unit and instrument level testing.
- This +/-3.3% cooler hold time uncertainty translates into +/- 1uW cooler total load uncertainty (based on a 30uW total cooler load [AD1]).

Table 3-1 shows the cooler total parasitic load predicted with the thermal model versus the ones measured at unit level for two thermal environments, 1.6K/1.8K and 1.7K/4K respectively.

| L0 / L1 Thermal Environments | 1.6K / 1.8K | | 1.7K / 4K | | Correlation Factor |
|---|---|---|---|---|---|
| | Measured | Predicted | Measured | Predicted | |
| L1 Kevlar Parasitic [uW] | - | 0.24 | - | 1.534 | - |
| Shunt Parasitic [uW] | - | 4.906 | - | 5.738 | 1.3795 |
| Heat Switch [uW] | - | 3.472 | - | 4.061 | 0.8 |
| Total Parasitic [uW] | 6.9 | 8.618 | 11.3 | 11.33 | - |
| Agreement | + 24.9% | | + 0.3% | | - |

*Table 3-1 – Correlated Cooler TMM Predictions versus Cooler Performances measured at Unit Level*

A 1.3795 correlation factor was applied on the evaporator heat switch OFF conductance in order to match the unit level test result. No test data were available to cross check the parasitic load from the shunt titanium tube. A 0.8 factor was applied to the shunt tube conductance to match the total parasitic load measured at unit level for the 1.7K/4K test case.

The analyses show that while the correlated model is in good agreement with the measured performances for the 1.7K/4K environment but higher discrepancies have been noted for the 1.6K/1.8K case. These are probably linked to higher uncertainties in the data used for the titanium thermal conductivity for the 0.2K-0.3K range i.e. the titanium thermal conductivity has been assumed constant within this range. Note: Lionel Duband's theoretical model predicted a total parasitic load of 8.5uW for the 1.6K/1.8K test case [RD2]. This value is within 1.3% of the data predicted by the RAL thermal model and therefore in good agreement despite the discrepancy with the actual measured value.

### *3.4.2 Sorption Cooler Model – Hold time Predictions*

Another important aspect of the cooler thermal model correlation is the validation of the cooler hold time prediction based on:

- Cooler initial Helium3 charge: 6.3L,
- Evaporator total operational heat load,
- Evaporator temperature at end of condensation phase,
- Pump temperature at end of condensation phase,
- Condensation efficiency (based on the evaporator temperature at the end of the condensation phase),
- Cryo-pumping efficiency (based on the evaporator temperatures at the end of both the condensation and the cryo-pumping phase),
- Latent heat of evaporation based on the evaporator cold base temperature.

Table 3-2 describes the cooler hold times measured at unit level for different test cases [RD2] and the hold time predicted by the thermal model for the same evaporator total load and temperature of condensation.

| | Units | Case1 | Case2 | Case1-2 | Case2-2 | Case 3 |
|---|---|---|---|---|---|---|
| **L1 / L0 Thermal Environment** | **[K]** | **1.6K / 1.8K** | | | | **1.7K / 4K** |
| Evaporator Parasitic Load | [uW] | 6.87 | 6.87 | 6.87 | 6.87 | 11.30 |
| Evaporator Applied Load | [uW] | 200.00 | 30.00 | 200.00 | 30.00 | 10.00 |
| Evaporator Total Load | [uW] | 206.87 | 36.87 | 206.87 | 36.87 | 21.30 |
| Temperature of Evaporator at End of Condensation | [K] | 2.15 | 2.15 | 2.1 | 2.1 | 2.1 |
| Temperature of Pump at End of Condensation | [K] | 45 | 45 | 45 | 45 | 45 |
| Measured Hold Time at Unit Level | [hr] | 7.07 | 39.63 | 7.08 | 40.45 | 69.08 |
| Estimated Hold Time with TMM | [hr] | 7.16 | 38.34 | 7.30 | 39.10 | 67.01 |
| Agreement | [%] | -1.3 | 3.3 | -3.1 | 3.3 | 3.0 |

*Table 3-2- Measured versus Predicted Cooler Hold Time for Unit Level Testing*

The model agrees with the measured data to within +/-3% which is consistent with the level of accuracy obtained during the unit level testing.

### *3.4.3 300mK Busbar Assembly*

An important aspect of the 300mK busbar is the validation of the temperature gradient along the various sections of the strap during the low temperature operation phase at 300mK. This depends on the following parameters:

- BDA parasitic load, from 1.7K to 0.3K,
- Busbar parasitic load, from 1.7K to 0.3K,
- Copper thermal conductivity at 0.3K,
- Interface thermal conductance at 0.3K.

Many aspects of the busbar thermal performance have been characterised at unit level at 300mK (i.e. thermal conductivity of copper and interface conductances). These have been summarised in [RD4] and have been used as an input when updating the thermal model. The assumptions used to model the busbar parasitic heat load (through the Kevlar supports) are believed to be accurate (to within 6% [RD3]) as similar to the cooler Kevlar supports.

The correlation of the busbar depends on the following parameters:

- Temperature measurements at the evaporator cold tip and at each BDA,
- 300mK system total parasitic load at the time the temperatures were measured.

Temperature measurements during the PFM2 and PFM3 test campaign were found to be inconsistent and therefore prevented the correlation of the Busbars. Most of the material and interface conductance had been characterised at unit level however, thus giving good confidence about the assumptions used for the modelling.

Some analysis was performed using the thermal model (with correlated BDA parasitic load and internal temperature gradients) for the photometer BDAs using test data from the PFM2 and PFM3 test campaigns.

| | | PFM2 | TMM Prediction for PFM2 Environment | Delta |
|---|---|---|---|---|
| **Node** | **ID** | **mK** | **mK** | **mK** |
| 4300 | Evap | **288.5** | 288.5 | 0 |
| 2750 | PLW | **293** | 304.5 | 11.5 |
| 2850 | PMW | **298** | 306.3 | 8.3 |
| 2950 | PSW | **300** | 307.5 | 7.5 |
| | | | Mean Deviation | **9.1** |

*Table 3-3 – Predicted Photometer BDAs temperature for PFM2*

A mean deviation of 9.1mK was found between the measured BDA temperatures and the ones predicted with the thermal model. When this 9.1mK is applied to the cooler cold tip, a correlation of the BDA temperatures can be achieved to within -1.6mK/2.4mK as described in the following table. An adequate temperature drop along the BDA and busbar is also obtained.

| Updated Cooler Cold Tip | Correlation | Temperature Drop busbar+ inside BDA | Internal BDA | Busbar |
|---|---|---|---|---|
| **mK** | **mK** | **mK** | **mK** | **mK** |
| **279.4** | - | - | - | - |
| 295.4 | 2.4 | 16.0 | 7.48 | 8.52 |
| 297.2 | -0.8 | 17.8 | 10.28 | 7.52 |
| 298.4 | -1.6 | 19.0 | 11.6 | 7.4 |

*Table 3-4 – Updated Predictions for Photometer BDAs temperature for PFM2*

The same approach was used for the PFM3 test data as described in the table below. In this case, a mean deviation of 13.7mK was found between the measured BDA temperatures and the ones predicted with the thermal model.

| PFM3 | TMM Prediction for PFM3 Environment | Delta |
|---|---|---|
| **mK** | **mK** | **mK** |
| **288.5** | 288.5 | 0 |
| **292.3** | 304.5 | 12.2 |
| **291** | 306.3 | 15.3 |
| **294** | 307.5 | 13.5 |
| | Mean Deviation | **13.7** |

*Table 3-5 – Predicted Photometer BDAs temperature for PFM3*

When this 13.7mK is applied to the cooler cold tip, a correlation of the BDA temperatures can be achieved to within -1.5mK/2.0mK as described in the following table.

| Updated Cooler Cold Tip | Correlation | Temperature Drop busbar+ inside BDA | Internal BDA | Busbar |
|---|---|---|---|---|
| mK | mK | mK | mK | mK |
| 274.8 | - | - | - | - |
| 290.8 | -1.5 | 16 | 7.48 | 8.52 |
| 292.6 | 1.6 | 17.8 | 10.28 | 7.52 |
| 293.8 | -0.2 | 19 | 11.6 | 7.4 |

*Table 3-6 – Updated Predictions for Photometer BDAs temperature for PFM3*

This analysis suggests that an offset error of 9-14mK is present in the measurements of the 300mK system temperatures. During the PFM4 test campaign, the evaporator temperature sensor was checked for self-heating with a GSE AC bridge. The excitation current to the sensor was varied from 3.16nA to 31.6nA, the self-heating was recorded and the sensor interface conductance estimated. In flight, the evaporator is driven with a constant AC excitation current of 40nA. Based on the characterized sensor interface, the self-heating error of the temperature sensor has been estimated to be ~11mK for the prime sensor and ~13mK for the redundant sensor. This is consistent with the thermal model predictions of a 9mK-14mK constant error offset (as presented at the SVR2 [RD10]). This therefore means that the actual cold tip temperature for a 1.7K/4.3K environment is closer to ~278mK (than the measured 288.5mK) and that the photometer busbar temperature drop is likely to be about 10mK.

### *3.4.4 Bolometer Detector Arrays*

An important aspect of the Bolometer Detector Arrays (BDA) thermal model correlation is the validation of their total parasitic load and internal temperature gradient during the low temperature operation phase at 300mK. This depends on the following parameters:

- Kevlar supports parasitic load, from 1.7K to 0.3K,
- Kapton Harnesses parasitic load, from 1.7K to 0.3K,
- Internal construction (gradients) of BDA at 300mK.

The thermal model of each BDA (five in total) was updated to reflect the design parameters described in [RD5] and correlated against Unit Level test data (for parasitic load and internal temperature gradient) [RD6].

The following thermal model was used for the correlation:
J:\TD-01-02-SPIRE\DTMM\SPIRE_TMM_STAL_3-2\ SPIRE_TMM_FM_2-4s2.d

The correlation results can be found at:
J:\TD-01-02-SPIRE\DTMM\SPIRE_TMM_STAL_3-2\Results\BDA

The BDA thermal model parasitic load was first correlated against the EIDP values. Only the parasitic loads from the Kapton harnesses were adjusted as part of the correlation as these have the most uncertainties associated with them i.e. the parasitic from the Kevlar cord are believed to be well characterised (similar to the ones used on the cooler). The correlation was

achieved by setting the BDA L0 and 300mK interfaces as boundaries to 1.7K and 300mK respectively.

| | BDA | BDA Harnesses # | BDA Parasitic Load From EIDP | TMM Uncorrelated Parasitic Load | Predicted Reqd Factors on Harnesses | Correlated TMM Parasitic Load | Ratio |
|---|---|---|---|---|---|---|---|
| **Node** | | | uW (1) | uW (2) | - | uW (2) | - |
| **2700** | **PLW** | 2 | 2.1 | 2.433 | **0.87** | 2.312 | 1.10 |
| **2800** | **PMW** | 4 | 2.3 | 3.357 | **0.55** | 2.526 | 1.10 |
| **2900** | **PSW** | 6 | 3.9 | 4.276 | **1.00** | 4.276 | 1.10 |
| **3700** | **SLW** | 1 | 2.9 | 1.968 | **3.51** | 3.131 | 1.08 |
| **3800** | **SSW** | 2 | 2.1 | 2.433 | **0.87** | 2.312 | 1.10 |
| | Total | 15 | 13.3 | 14.47 | | 14.557 | 1.09 |

*Table 3-7 – BDA Internal Parasitic Load Correlation*

*(1) EIDP for 1.7K, 300mK boundaries*
*(2) For node NXX00 and NXX10 held at 1.7K, 300mK boundaries*
*(3) Delta between NXX10 and NXX50*

The factors described in Table 3-7 have been applied to the BDA Kapton harness overall conductance. A 10% correlation of the BDA total parasitic load has been achieved.

Known limitation: The Kapton harnesses conductances have not been modelled with temperature dependent data in the model.

Then the BDA internal temperature drop was correlated against the EIDP values. The interface conductance between the detector cover and the feed horns was adjusted as this is where the internal drop is most likely to take place. Again, the correlation was achieved by setting the BDA L0 and 300mK interfaces as boundaries to 1.7K and 300mK respectively.

| BDA Internal Drop From EIDP | TMM uncorrelated Internal Drop | Predicted Reqd Factors on IF between Feedhorn and Cover | Correlated TMM Internal Drop | Delta T |
|---|---|---|---|---|
| mK (1) | mK (2,3) | **Corr Fac** | mK (2,3) | mK |
| 7.0 | 8.4 | **1.20** | 7.2 | 0.20 |
| 10.0 | 9.3 | **0.93** | 9.9 | -0.10 |
| 9.8 | 17.9 | **1.83** | 11.15 | 1.35 |
| 11.6 | 12.4 | **1.07** | 11.788 | 0.19 |
| 7.2 | 8.3 | **1.15** | 7.4 | 0.20 |

*Table 3-8– BDA Internal Temperature Drop Correlation*

*(1) EIDP for 1.7K, 300mK boundaries*
*(2) For node NXX00 and NXX10 held at 1.7K, 300mK boundaries*
*(3) Delta between NXX10 and NXX50*

Correlation factors ≤ 20% were required in most cases with the exception of PSW where a lower correlation agreement was obtained.

## 3.5 Validation of the L0 Detector Enclosure Stage

### *3.5.1 L0 Interbox Strap and SST L0 Supports Parasitic Load*

The L0 interbox strap has been characterised as part of the CQM2 test campaign. The following limitations were applicable:

- The SST L0 supports were fitted (CFRP supports are now part of the baseline),
- New interbox strap implemented (with glued isolation pads),
- Two sensors were fitted on each L0 enclosure - one EGSE sensor near the interbox strap interface and one Flight sensors at one of the L0 support interface,
- The EGSE sensor near the interbox strap interface on the spectrometer was lost during the test campaign,
- Another EGSE sensor was fitted on the L0 strap adaptor,
- During the characterisation test, the data from the various temperature sensors were found to be inconsistent,
- It was later found that the flight temperature sensor had a DC offset error [RD8]. They were therefore left out in subsequent analysis of the CQM2 data,
- Another attempt at this characterisation was planned for the PFM2 test campaign (with the CFRP feet) but the EGSE heater was found open circuit after cooldown.

*Summary of CQM2 Characterisation test and inputs to thermal correlation*

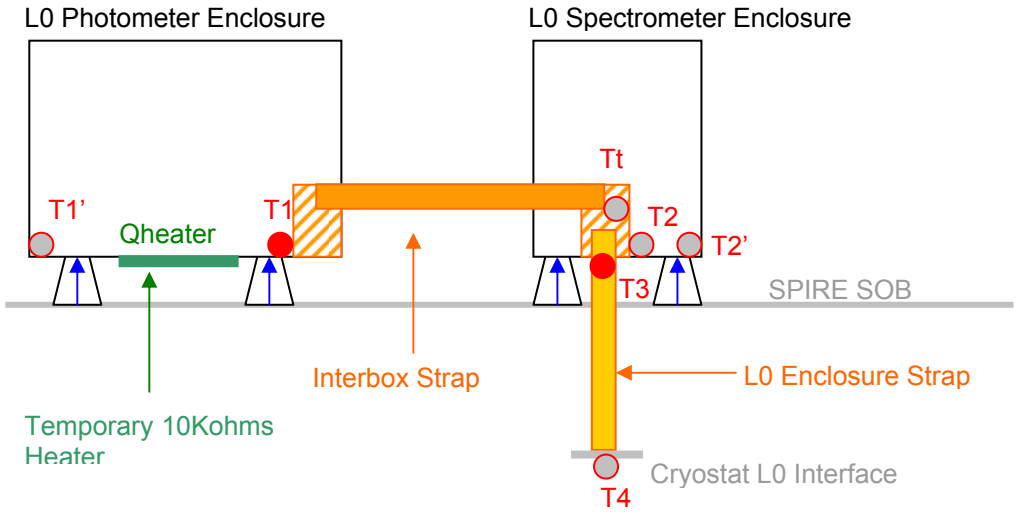


Working Sensors

Non Working Sensors

Enclosure Parasitic Heat Load through SST supports and harnesses

Notes:

- T1' and T2' were flight sensors and are therefore discarded because of the DC offset error,
- T2 was lost during cooldown,
- T4 was lost during cooldown (and found to be out of calibration when working during the PFM2 test campaign),

- Only T1 and T3 were available for the correlation,
- The heater was glued on Kapton tape which was then fitted on the photometer enclosure. This approach had the advantage that the heater could be removed at later stage.

Table 3-9 summarises the setup of the heater mounted on the L0 photometer enclosure during the interbox strap characterisation test.

| Required Dissipation | Commanded Current | Measured Voltage | Actual Dissipated Power |
|---|---|---|---|
| [mW] | [mA] | [V] | [mW] |
| 0 | 0 | 0 | 0 |
| 5 | 0.7 | 6.95 | 4.865 |
| 10 | 1 | 9.9 | 9.9 |

*Table 3-9 – Heater Test Setup for L0 Enclosure Characterisation*

| Temperature Sensors | ID | 0 mW Case | 5 mW Case | 10mW Case | Comments |
|---|---|---|---|---|---|
| **Date** | **-** | **14/09/2000 21:45** | **14/09/2000 20:37** | **14/09/2000 19:00** | **-** |
| Photo at PLW IF | T1' | 1.721 | 2.065 | 2.344 | DC Offset |
| Photo at Strap IF | T1 | 1.764 | 1.938 | 2.101 | ✓ |
| Spectro IF at A Frame | T2' | 1.677 | 1.782 | 1.87 | DC Offset |
| Spectro at Strap IF | T2 | - | - | - | Open Circuit |
| L0 Enclosure Strap Adaptor | T3 | 1.728 | 1.798 | 1.869 | ✓ |
| Enclosure Cryostat L0 IF | T4 | - | - | - | Open Circuit and Out of Calibration |

*Table 3-10 - Interbox L0 Strap Characterisation Test – Results*

*Overview of the correlation method description*

Definition of the unknown:
- Overall Interbox strap conductance (glued pad + bolted interface + strap + bolted interface), defined as G2,
- Interface conductance between the L0 strap and the spectrometer copper pad, defined as G1,
- Photometer SST support and F-harnesses parasitic load, defined as Qp,
- Spectrometer SST support and F-harnesses parasitic load, defined as Qs.

Known Variables:
- Interbox and pad copper thermal conductivity as a function of temperature [RD4],
- Glued joint conductance as a function of temperature [RD4],
- Cu/Cu bolted joint conductance as a function of temperature [RD4],
- Photometer heater dissipation using 4-wire measurement defined as Qh.

| Test Case | 1 | 2 | 3 |
|---|---|---|---|
| **Q_Heater [mW]** | **0** | **4.865** | **9.9** |
| T3 at L0 Enc strap adaptor [K] | 1.728 | 1.7985 | 1.869 |
| T1 at Phot Strap I/F [K] | 1.7639 | 1.938 | 2.100 |
| **Conductances [W/K]** | | | |
| Glued IF at T1 | 0.6381 | 0.8216 | 0.9924 |
| Pad at T1 | 1.9304 | 2.1209 | 2.2982 |
| Bolted IF at T1 | 0.2074 | 0.2279 | 0.2470 |
| Interbox Strap at Tavr | 0.4815 | 0.5152 | 0.5473 |
| Bolted IF at T2 | 0.2032 | 0.2115 | 0.2198 |
| Pad at T2 | 1.8911 | 1.9683 | 2.0454 |
| Pad at T2 | 0.3362 | 0.3499 | 0.3636 |
| Bolted IF at T2 | 0.2032 | 0.2115 | 0.2198 |
| G1_Overall Conductance [W/K] | 0.2032 | 0.2115 | 0.2198 |
| G2_Overall Conductance [W/K | 0.0558 | 0.0602 | 0.0641 |

*Table 3-11 – G1 and G2 overall conductances versus temperature*

(*) with bolted interface conductance assumed to follow a linear fit of 0.2xT,
(**) A curve fit of test data (see below) has been used for the Stycast glued joint conductance in order to get temperature dependent performance.

| T | k_stycast |
|---|---|
| 1.730 | 0.022 |
| 1.912 | 0.028 |
| m | p |
| 0.03778 | -0.04377 |

*Table 3-12 – Stycast Glued Joint Interface Conductance curve fit*

*Mathematical Expressions and Assumptions Used:*

- Assume Tt the (virtual) temperature on the Spectrometer pad,
- It is assumed that the photometer and spectrometer SST supports and the F-harnesses are of identical built standard (in terms of materials used and manufacturing/construction processes i.e. only numbers of harnesses and the support geometry differ, both of which are well known). Therefore any correlation factor that would apply to the photometer parasitic load would also apply to the spectrometer parasitic load.
- Based on predictions with the uncorrelated model (and with the L1 and L0 set to 4.5K and 1.7K respectively) the breakdown between the photometer L0 enclosure parasitic load and the L0 spectrometer enclosure was found to be 0.337 i.e. Qs = 0.337 x Qp. This breakdown will be used to reduce the number of unknown when completing the correlation.
- The conductance of G1 and G2 have been estimated using best information available to date about material properties and as a function of T1 and T3, as described in table 4.11.

- A factor to account for the reduction in L0 enclosure parasitic loads as the delta T between the L1 and L0 temperature stage reduces (i.e. the L0 warms up when higher heater power dissipations are used) has also been accounted for, Qp_fac.

Then the following expressions have been used to solve for Qp:

$(Qp + Qh) / G2 = T1 - Tt$ (1)

$(Qp + Qh + Qs) / G1 = Tt - T3$ or $(Qp + Qh + 0.337 \times Qp) / G1 = Tt - T3$ (2)

Expression (3) is then obtained by adding (1) + (2):

$Qp = [ (T1 - T3) \times (G1 \times G2) - Qh \times (G1 + G2) ] / [ T\_Fac \times (G1 + G2 + 0.337 \times G2) ]$ (3)

- Expression (3) was computed with the data from the test cases 2 and 3 (i.e. the temperature gradient for case 1 would be too small to provide a good correlation and a two point fit was used instead with maximum of 7.2% error ~ 0.11mW).
- Then the bolted conductance G1 (and indirectly G2 which also includes two bolted interfaces) was varied iteratively in order for the expression 3 to converge towards an identical value for Qp.

*Summary of Correlation Analysis:*

| | Case 1 | Case 2 | Case 3 |
|---|---|---|---|
| Qh Photometer Heater [mW] | 0 | 4.865 | 9.9 |
| Temperature at the L0 Enclosure Strap Adaptor [T3] | 1.728 | 1.7985 | 1.869 |
| Temperature at the Photometer Strap Interface [T1] | 1.7639 | 1.938 | 2.100 |
| G1 Estimated Conductance [W/K] | 0.3456 | 0.3597 | 0.3738 |
| G2 Estimated Overall Conductance [W/K] | 0.0718 | 0.0777 | 0.0830 |
| Parasitic Load Temperature Factor [T_Fac] | 1 | 0.94 | 0.88 |

*Table 3-13 – Nominal Temperature and conductance used for iteration*

The test data converged for a 0.588 degradation factor applied to the nominal 0.2xT bolted interface conductance, as described in table below:

| Case | T1 | T3 | G1 | G2 | Qs_fac | Qp_fac | Qh | Qp |
|---|---|---|---|---|---|---|---|---|
| 5mW | 1.938 | 1.799 | 0.212 | 0.060 | 0.337 | 0.936 | 4.865 | 1.659 |
| 10mW | 2.100 | 1.869 | 0.220 | 0.064 | 0.337 | 0.877 | 9.900 | 1.659 |

*Table 3-14 - Degradation Factor: 0.588 – two similar values are obtained for Qp (data converged)*

*Summary of correlation:*

- The characterised photometer parasitic heat load is 1.659mW (SST supports + harnesses) for a 1.7K/4.5 environment,
- The characterised spectrometer parasitic heat load is 0.337 x 1.659 = 0.559 mW (supports + harnesses) for a 1.7K/4.5K environment,
- The characterised total L0 parasitic heat load is 0.559 + 1.659 = 2.22 mW (SST supports + harnesses) for a 1.7K/4.5K environment,
- A predicted total L0 parasitic heat load of 2.1mW (SST supports + harnesses) was obtained with the thermal model for a 1.7K/4.5 environment, showing a 95.4% agreement with the characterised model.
- The bolted interface conductance is predicted to follow the following degraded linear law: 0.2 x 0.588 x T = 0.1176 x T i.e. G = 0.2 W/K at 1.7K.
- The interbox strap overall conductance is described in the figure below.

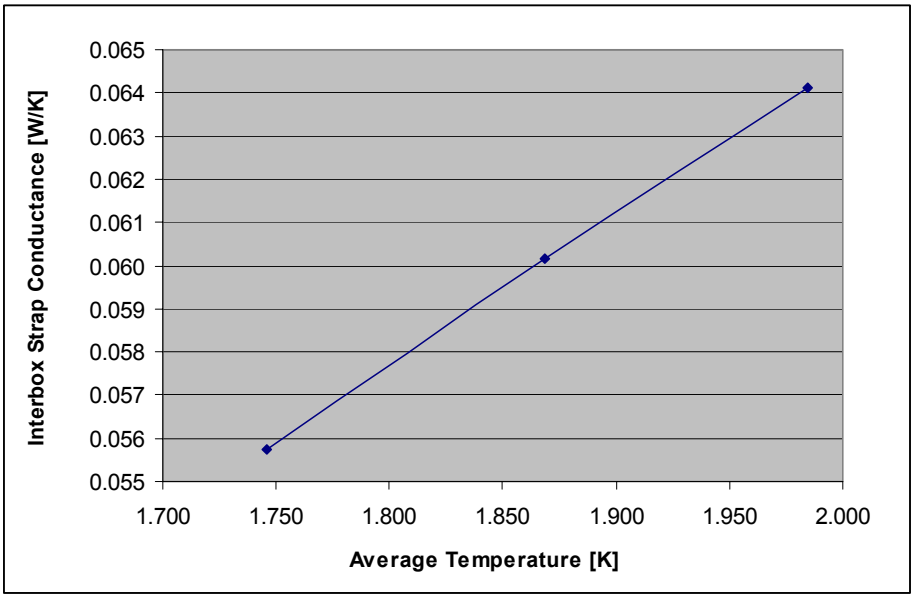


*Figure 3-1 – L0 Interbox Strap Conductance*

### *3.5.2 Flight CFRP L0 Supports and Parasitic Load*

The CFRP L0 supports were implemented and tested for the first time during the PFM2 test campaign. The thermal conductivity of the CFRP has been measured at unit level (for a 5K to 11K range) as described in the figure below. The data has been extrapolated from 11K up to 16K and the thermal conductivity of the HM type perpendicular was used for the temperature below 5K.

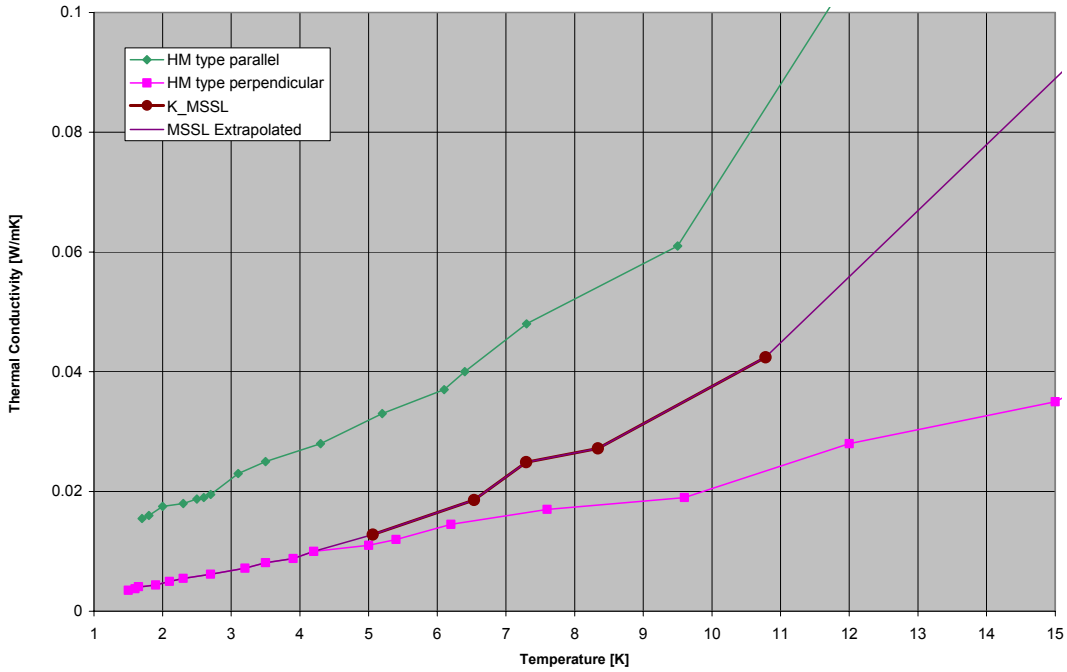


*Figure 3-2 –Thermal Conductivity of CFRP used by MSSL for design of L0 and L1 Supports*

Two thermal balance test cases were carried out as part of the PFM2 test campaign [RD8] with a cold and hot L0 and L1 thermal environments. The results from these tests were used to correlate the conductance of the L0 CFRP supports with the thermal model. Table 3-15 shows the L1 and L0 temperatures measured (and then corrected for the DC offset) during the PFM2 cold thermal case as well as their equivalent node number in the thermal model. The last column of the table describes which thermal nodes were held as a boundary as well as the predicted temperature for the L0 enclosures (modelled as diffuse nodes). A good level of agreement was obtained with a factor 2 applied to the CFRP isolation support conductance. A similar level of agreement was obtained for the hot case as described in Table 3-16. Based on this correlation, a factor 2 has therefore been applied to all CFRP supports in the thermal model.

| | DTMM node | PFM2 Measured | PFM2 Corrected (*) | TMM Predictions |
|---|---|---|---|---|
| Spectrometer L0 Enclosure (near strap interface) | 2400 | 1.707 | 1.711 | 1.710 |
| Photometer L0 Enclosure (near strap interface) | 3400 | 1.719 | 1.715 | 1.715 |
| T_FPU_MYAF | 1600 | 4.344 | 4.344 | B |
| T_FPU_PYAF | 1500 | 4.362 | 4.362 | B |
| T_SOB_CONE | 1300 | 4.369 | 4.369 | B |
| SOB L1 Strap IF | 1130 | 4.275 | 4.275 | B |
| L0 Enclosure Adaptor | 6100 | 1.707 | 1.707 | B |
| L0 Pump Adaptor | 6200 | 1.764 | 1.764 | B |
| L0 Evaporator Adaptor | 6300 | 1.702 | 1.702 | B |

*Table 3-15 – SPIRE Thermal Model Correlation of CFRP L0 Supports Conductance for Cold Case*

| | DTMM node | PFM2 Measured | PFM2 Corrected (*) | TMM |
|---|---|---|---|---|
| Spectrometer L0 Enclosure (near strap interface) | 2400 | 1.936 | 1.941 | 1.942 |
| Photometer L0 Enclosure (near strap interface) | 3400 | 1.954 | 1.949 | 1.950 |
| T_FPU_MYAF | 1600 | 5.230 | 5.230 | B |
| T_FPU_PYAF | 1500 | 5.244 | 5.244 | B |
| T_SOB_CONE | 1300 | 5.642 | 5.642 | B |
| SOB L1 Strap IF | 1130 | 4.798 | 4.798 | B |
| L0 Enclosure Adaptor | 6100 | 1.939 | 1.939 | B |
| L0 Pump Adaptor | 6200 | 1.992 | 1.992 | B |
| L0 Evaporator Adaptor | 6300 | 1.932 | 1.932 | B |

*Table 3-16 -SPIRE Thermal Model Correlation of CFRP L0 Supports Conductance for Hot Case*

(*) corrected for DC offset

### 3.6 Validation of the Flight L0 Thermal Straps

The thermal conductance of the SPIRE FM L0 thermal strap has been measured at unit level and the following conductance were obtained [RD11]:

L0 detector strap ~ 210 mW/K at 1.7K
L0 pump strap ~ 145 mW/K at 1.7K
L0 evap strap ~ 140 mW/K at 1.7K

These measurements do not include the bolted interface conductance at the cooler heat switches or at the spectrometer enclosure but they do include the bolted interface with the spacecraft.

According to the Herschel thermal model (issue 4.6), the bolted interface conductance of each strap with the spacecraft is ~ 2.37 W/K at 1.7K. Based on the L0 interbox strap correlation, it is assumed that the bolted interface conductance to the spectrometer enclosure and cooler heat switches follows the linear law 0.1176 x T (~ 0.2W/K at 1.7K). Using these data, the conductance of the L0 straps has been estimated (excluding the bolted interface at the spacecraft end which is already included in the Herschel thermal model).

| Conductance [W/K] | Measured At Unit Level | Strap conductance excluding the spacecraft Interface | Strap conductance excluding the spacecraft Interface but Including the cooler/spectrometer interface |
|---|---|---|---|
| L0 Spectrometer Strap | 0.210 | 0.230 | 0.107 |
| L0 Evaporator Strap | 0.140 | 0.149 | 0.085 |
| L0 Pump Strap | 0.145 | 0.154 | 0.087 |

*Table 3-17 – Predicted thermal conductance of the SPIRE L0 Thermal Straps*

## 3.7 Validation of Instrument Power Dissipation at L1

### *3.7.1 PCAL Operation*

The photometer calibration source (PCAL) dissipated 2.91mW for 30 sec every hour [RD9], this corresponds to a hourly average dissipation of 24.3uW.

| Measured Source Voltage | Measured Source Bias | Peak Power | Average Power [*] |
|---|---|---|---|
| [V] | [mA] | [mW] | [mW] |
| 0.769 | 3.8 | 2.91 | 0.024 |

*[*] 0.83% duty cycle*

*Table 3-18 – PCAL Operation during PFM3 test campaign [RD9]*

Note: PCAL is in operation both in photometer and spectrometer mode.

### *3.7.2 SCAL Operation*

The baseline is to warm the spectrometer calibration source (SCAL) to a temperature that matches the Herschel telescope's temperature while in flight. The baseline was for SCAL to be warmed to 80K, the current predictions with the Herschel thermal model (Issue 4.6) show the telescope mirrors temperatures ranging between ~79.3-79.7K. The tables below shows the power required to hold the SCAL2 at a given temperature as measured during the PFM3 test campaign at RAL [RD9]. A peak power of 15mW allows the SCAL to reach 86K within a period of 3.5 min.

| Measured Source Voltage | Measured Source Bias | ON Peak Power | Average Power Hourly Duty Cycle | Average Power 46hr Duty Cycle |
|---|---|---|---|---|
| [V] | [mA] | [mW] | [mW] | [mW] |
| 2.75 | 5.499 | 15.1 | 0.87mW | 0.019 |

*Table 3-19 – SCAL2 Operation during PFM3 test campaign [RD9]*

| Measured Source Voltage | Measured Source Bias | Power | Comment |
|---|---|---|---|
| [V] | [mA] | [mW] | - |
| 0.630 | 1.259 | 0.79 | SCAL2 @ 49.2K |
| 1.009 | 2.018 | 2.04 | SCAL2 @ 80.8K |
| 1.095 | 2.190 | 2.40 | SCAL2 @ 86K |

*Table 3-20 – SCAL2 Operation during PFM3 test campaign [RD9]*

### 3.7.3 SMEC Operation

#### 3.7.3.1 Definition of Operating Modes

The table below summarises the possible scanning modes when the SMEC is in operation.

| Resolution | Low (L0) | Medium (MED) | High (HI) |
|---|---|---|---|
| **Range wrt ZPD** | +/- 1mm | +/- 3.4mm | -7/+31.5 |
| **Range** | 7mm to 9 mm | 4.76mm to 11.4mm | 1mm to 39.5mm |
| **Scan type** | Triangular | Triangular | Triangular |
| **Scan speed** | 0.5 mm/s | 0.5 mm/s | 0.5 mm/s |

*ZPD is at 8mm*

*Table 3-21- SMEC Scanning Modes*

#### 3.7.3.2 Verification of SMEC PFM Coil Resistance

The resistance of PFM SMEC coils could be verified during the PFM4 test campaign [RD12] while the SMEC was operated in High Resolution mode (where the peak current and voltage measurements are the most accurate). A plot of the PFM SMEC current, voltage and power dissipation is presented in the figure below and shows that for an average FPU temperature of 5.4K, the SMEC coil resistance is closed to ~4 ohms (i.e. 3.7 ohms has been measured at unit level on CQM SMEC for a similar hardware [RD13]).

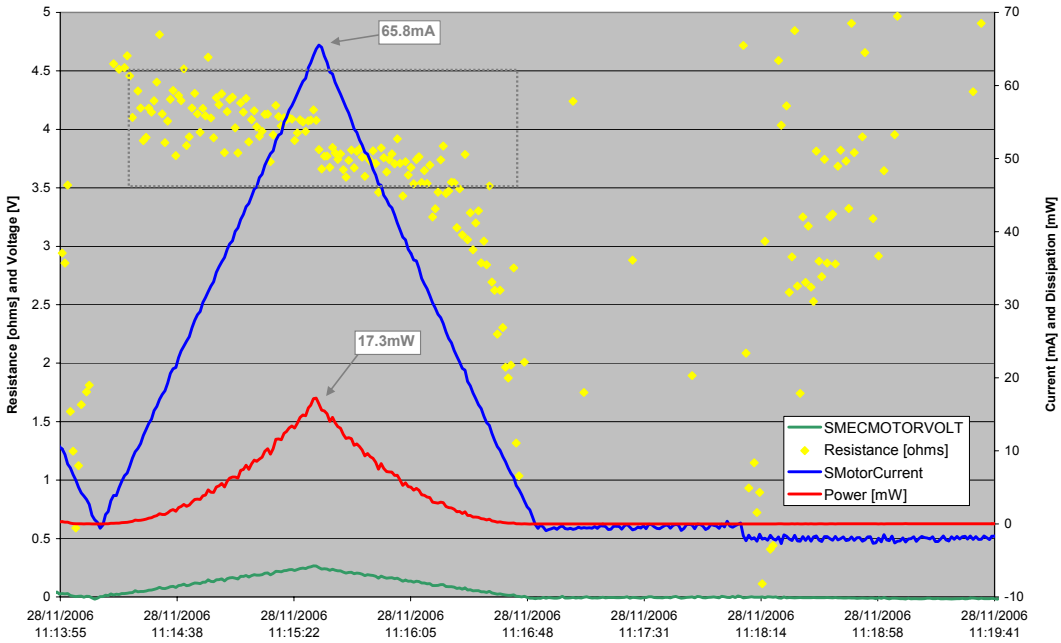


*Figure 3-3 – SMEC Current, Voltage and Power Dissipation in High Resolution Scan Mode [RD12]*

Note: Power dissipation profile is non linear over full scanning range.

#### 3.7.3.3 Verifications of SMEC PFM Power Dissipation

The SMEC linear law is calculated based on the SMEC maximum displacement (39.5mm) in High (HI) resolution mode and the measured high peak current, as described in the table below.

| Mode | Max Range Displacement | Measured Peak Current | Linear Law |
|---|---|---|---|
| - | mm | mA | - |
| HI | 39.5 | 65.8 | 1.6658 |

*Table 3-22 - SMEC Current vs Displacement Linear Law*

This linear law can then be used to predict the peak currents for the lower resolution modes based on their maximum displacement. Please note that a 4 ohms coil resistance has been assumed for the calculations of the power dissipations (i.e. the measured voltage/current signals become too noisy to allow the calculation of the dissipated power).

| Mode | Max Range Displacement | Estimated Peak Current |
|---|---|---|
| - | mm | mA |
| MED | 11.4 | 19 |
| LO | 9 | 15 |

*Table 3-23 – SMEC Peak Current in MED and LO Resolution Scanning Mode*

The figure below describes the SMEC current and position profiles during L0 and MED resolutions scans measured during PFM4 test campaign [RD12], one can see that the peak current are really close to the one predicted (within noise).

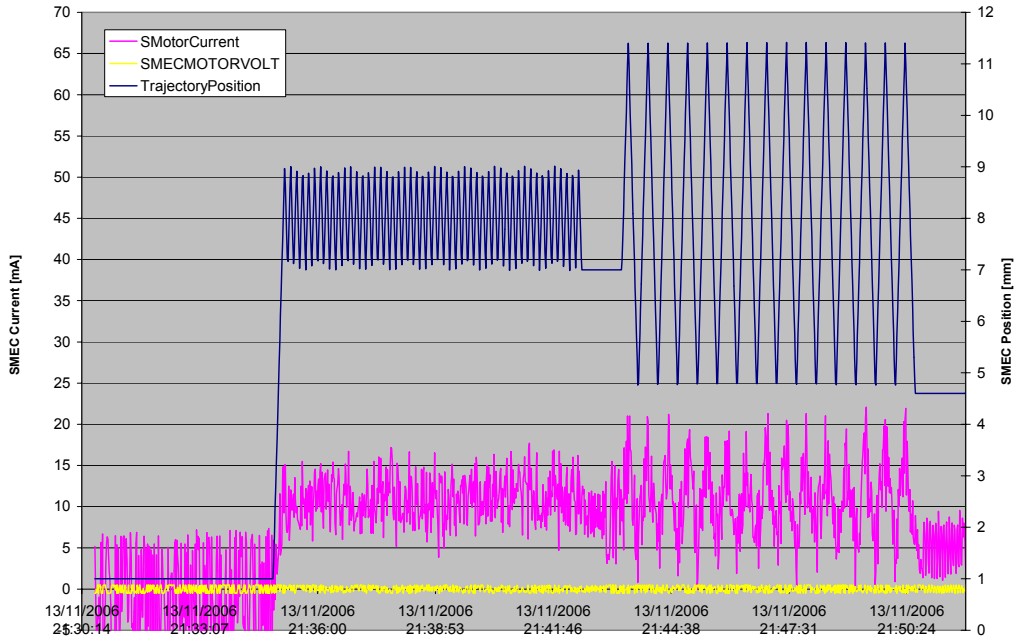


*Figure 3-4 - SMEC Current, Voltage and Scan Position in MED and LO Resolution Scan Modes [RD12]*

The table below summarises the predicted peak and average power dissipations for all three SMEC scanning modes.

| Mode | Peak Current | Peak Power | Average Power [*] | Duty Cycle in Spectrometer Mode |
|---|---|---|---|---|
| - | mA | mW | mW | % |
| LO | 15.0 | 0.90 | 0.43 | 33.3 |
| MED | 19.0 | 1.44 | 0.46 | 33.3 |
| HI | 65.8 | 17.3 | 3.56 | 33.3 |

*[*] Integrated over full displacement range for a single scan.*

*Table 3-24 – SMEC Average Power Dissipations*

### *3.7.4 BSM operation*

The PFM BSM performance has been measured at unit level [RD14], the table below summarises the main parameters performance.

| Parameters | Values | Units |
|---|---|---|
| Chop axis current law | 20.8 | mA/deg |
| Jiggle axis current law | 96.8 | mA/deg |
| Sensors | 0.8 | mW |
| BSM Coils Resistances | 0.85 | ohms |

*Table 3-25 – PFM BSM Performance*

Note: 0.85 ohms is a worse case as an average resistance of 0.82 ohms has been measured for the prime/redundant jiggle and chop motor coils resistances.

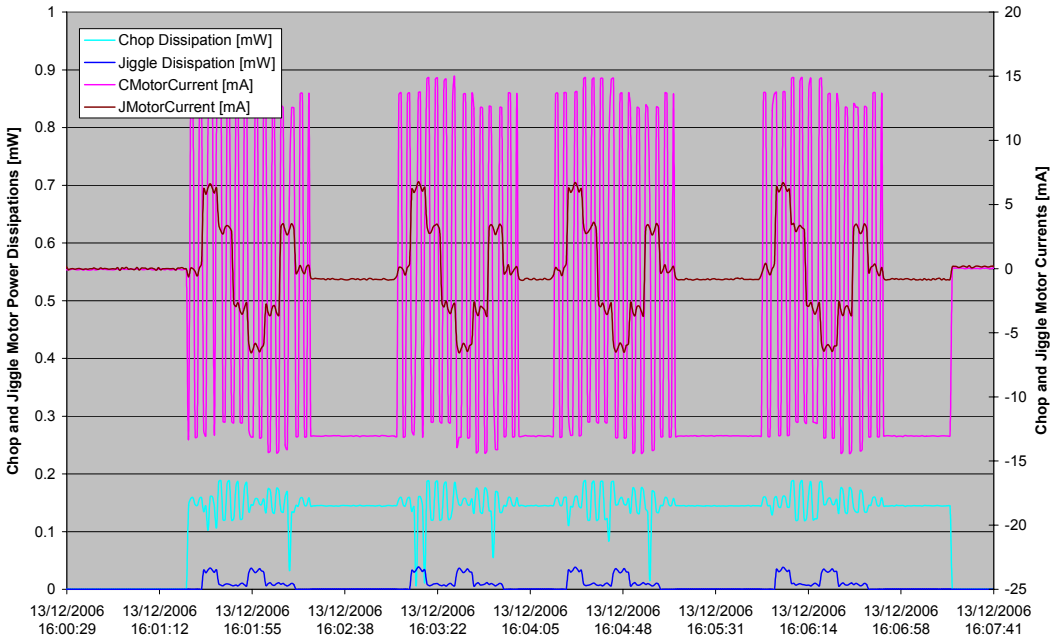


*Figure 3-5 - 7 point jiggle AOT performed during PFM4*

| BSM POWER DISSIPATION (mW) AT CHOP + JIGGLE COMBINATIONS : | | | | | | | | | | | | | | |
|---|---|---|---|---|---|---|---|---|---|---|---|---|---|---|
| MODE | | | JIGGLE | | | | | | | | | | | |
| | | | Angle | 0.573 | 0.52525 | 0.4775 | 0.42975 | 0.382 | 0.33425 | 0.2865 | 0.23875 | 0.191 | 0.14325 | 0.0955 | 0.04775 | 0 |
| | | | Current | 55.46464 | 50.84259 | 46.22053 | 41.59848 | 36.97643 | 32.35437 | 27.73232 | 23.11027 | 18.48821 | 13.86616 | 9.244107 | 4.622053 | 0 |
| | | | Power | 0.002615 | 0.002197 | 0.001816 | 0.001471 | 0.001162 | 0.00089 | 0.000654 | 0.000454 | 0.000291 | 0.000163 | 7.26E-05 | 1.82E-05 | 0 |
| CHOP | | | | | | | | | | | | | | |
| Angle | Current | Power | | | | | | | | | | | | |
| 2.53 | -52.65759 | 0.002357 | | 5.77 | 5.35 | 4.97 | 4.63 | 4.32 | 4.05 | 3.81 | 3.61 | 3.45 | 3.32 | 3.23 | 3.18 | 3.16 |
| 2.3 | -47.87053 | 0.001948 | | 5.36 | 4.95 | 4.56 | 4.22 | 3.91 | 3.64 | 3.40 | 3.20 | 3.04 | 2.91 | 2.82 | 2.77 | 2.75 |
| 2.07 | -43.08348 | 0.001578 | | 4.99 | 4.57 | 4.19 | 3.85 | 3.54 | 3.27 | 3.03 | 2.83 | 2.67 | 2.54 | 2.45 | 2.40 | 2.38 |
| 1.84 | -38.29643 | 0.001247 | | 4.66 | 4.24 | 3.86 | 3.52 | 3.21 | 2.94 | 2.70 | 2.50 | 2.34 | 2.21 | 2.12 | 2.06 | 2.05 |
| 1.61 | -33.50937 | 0.000954 | | 4.37 | 3.95 | 3.57 | 3.23 | 2.92 | 2.64 | 2.41 | 2.21 | 2.04 | 1.92 | 1.83 | 1.77 | 1.75 |
| 1.38 | -28.72232 | 0.000701 | | 4.12 | 3.70 | 3.32 | 2.97 | 2.66 | 2.39 | 2.15 | 1.96 | 1.79 | 1.66 | 1.57 | 1.52 | 1.50 |
| 1.15 | -23.93527 | 0.000487 | | 3.90 | 3.48 | 3.10 | 2.76 | 2.45 | 2.18 | 1.94 | 1.74 | 1.58 | 1.45 | 1.36 | 1.31 | 1.29 |
| 0.92 | -19.14821 | 0.000312 | | 3.73 | 3.31 | 2.93 | 2.58 | 2.27 | 2.00 | 1.77 | 1.57 | 1.40 | 1.28 | 1.18 | 1.13 | 1.11 |
| 0.69 | -14.36116 | 0.000175 | | 3.59 | 3.17 | 2.79 | 2.45 | 2.14 | 1.87 | 1.63 | 1.43 | 1.27 | 1.14 | 1.05 | 0.99 | 0.98 |
| 0.46 | -9.574107 | 7.79E-05 | | 3.49 | 3.08 | 2.69 | 2.35 | 2.04 | 1.77 | 1.53 | 1.33 | 1.17 | 1.04 | 0.95 | 0.90 | 0.88 |
| 0.23 | -4.787053 | 1.95E-05 | | 3.43 | 3.02 | 2.64 | 2.29 | 1.98 | 1.71 | 1.47 | 1.27 | 1.11 | 0.98 | 0.89 | 0.84 | 0.82 |
| 0 | 0 | 0 | | 3.41 | 3.00 | 2.62 | 2.27 | 1.96 | 1.69 | 1.45 | 1.25 | 1.09 | 0.96 | 0.87 | 0.82 | 0.80 |

*Figure 3-6 – BSM Power Dissipation at Chop and Jiggle Combinations [RD14]*

### 3.8 Validation of L1 Parasitic Load

A correlation of the L1 parasitic heat load could not be achieved very easily in the RAL calibration cryostat. The various loads making up the total L1 parasitic load are well understood however and/or conservative enough that the thermal model predictions should be accurate.

The SPIRE L1 parasitic load consists of:

- Parasitic load through the SST cone (x1) and CFRP A frames (x2) isolation supports – the modeling of the SST and CFRP supports has been validated by the correlation of the L0 enclosure parasitic loads.
- Parasitic load from the PJFET and SJFET harnesses – the PJFET harness heat load has been validated through the PJFET isolation support correlation. Similar assumptions have been used for the SJFET harnesses.
- Parasitic load from the housekeeping harnesses (Astrium's responsibility) – this is part of the Herschel thermal model and therefore isn't part of the SPIRE model correlation.
- The radiation load – a 0.2 emissivity has been used to model the SPIRE FPU enclosure. This assumption is believed to be conservative at these cryogenic operating temperatures.
- Internal power dissipation – the power dissipations from the various mechanisms and calibration sources has either been measured at unit level or as part of the instrument level test campaign at RAL.

The L1 isolation joint conductance has been characterized as part of the PFM3 test campaign [RD9] as being 0.74W/K at 1.7K, this represents a 0.14 degradation factor in comparison to the originally assumed 5.15W/K conductance.

### 3.9 Validation of JFET Boxes Performance

The PJFET isolation supports (and F-harness conductance) has been characterised as part of the CQM2 test campaign [RD7]. The table below describes the temperature of the nodes held as boundaries based on test data (in blues), the PJFET heater dissipation for each test case (in red) and in green the JFET chassis temperature (modelled as a diffuse node) as measured for each test case. The thermal model predictions and agreement are given in the last columns of the table. An acceptable level of correlation was achieved after a 1.1 factor was added to the PJFET isolation supports overall conductance.

| Q [mW] | PJFET Harness | PJFET HOB I/F | SOB L1 | FPU +Y | FPU -Y | FPU Cone | FPU L1 conn | PJFET Chassis | TMM Prediction | Delta |
|---|---|---|---|---|---|---|---|---|---|---|
| 0 | 18.795 | 15.329 | 4.379 | 4.559 | 4.630 | 4.684 | 4.497 | 16.762 | 16.750 | -0.012 |
| 20 | 21.237 | 15.539 | 4.370 | 4.555 | 4.633 | 4.684 | 4.513 | 20.901 | 20.970 | 0.069 |
| 40 | 23.668 | 15.492 | 4.405 | 4.590 | 4.679 | 4.720 | 4.567 | 24.312 | 24.340 | 0.028 |

*Table 3-26 – PJFET Correlation Overview*

The PJFET L3 isolation joint conductance has been characterized as part of the PFM4 test campaign [RD12] as being ~0.04W/K at 15K, this represents a 0.3 degradation factor in comparison to the originally assumed 0.138W/K conductance. In addition, a 0.333 degradation factor has also been added to the JFET chassis overall conductance based on the PFM4 test data.